CHyCle 2017

sciforum

Conference Proceedings Paper

Moisture transport related to the ENSO effects in the Mexican precipitation

Ana E. Melgarejo[1]*, Paulina Ordóñez[1], Raquel Nieto [2] , Luis Gimeno [2] and Pedro Ribera[3]

Published: 11/11/2017
Academic Editor: Francina Dominguez

[1] Centro de Ciencias de la Atmósfera. Universidad Nacional Autónoma de México. Cdmx, Mexico.
[2] EphysLab, Facultade de Ciencias, Universidade de Vigo, Ourense, Spain
[3] Dpto. Sistemas Físicos, Químicos y Naturales. Universidad Pablo de Olavide. Seville, Spain
* Correspondence: ann.ct@ciencias.unam.mx, Tel.: +52 1 55 5623 0222. Ext. 81879.

Abstract In the past, several works addressed the impact of El Niño-Southern Oscillation (ENSO) on Mexican precipitation by using relative scarce observations of the National Weather Service of Mexico or reanalysis data. In this work, we reassessed the ENSO signal in Mexican rainfall by using four precipitation databases (CHIRPS, GPCC, GPCP and CMAP) over a 34-yr period (1981-2014) and three different ENSO indices. Results obtained with different datasets are consistent among them and with previous studies, showing strong positive precipitation anomalies along the winter over the northern Mexico for El Niño events. In contrast, during the summer, negative rainfall anomalies can be found over most of central and southern Mexico, being stronger in August. During La Niña years, the anomalies show approximately the opposite pattern to those observed during El Niño.
A Lagrangian approach is used to track the evaporation minus precipitation (E-P) along trajectories followed by the atmospheric particles that will take precipitable water to the areas with a precipitation amount modulated by ENSO phases. Then, composites of the obtained (E-P) fields are examined for the strong phases of El Niño and La Niña. Finally, the synoptic conditions associated with ENSO-related anomalous atmospheric water vapor fluxes are studied for a better understanding of the origin of the ENSO impact on the Mexican precipitation.

Keywords: ENSO, Mexico, precipitation, moisture transport.

1. Introduction.

Mexico exhibits a monsoonal climate, with a rainy season concentrated during the boreal summer months and a relatively dry season in winter [1]. The country lies in a latitudinal belt that is sensitive to fluctuations in atmospheric circulation, i.e. northwards/southwards displacements of the Northern Hemisphere General Circulation [2]. In fact, the mexican climate is influenced by two dominant atmospheric circulation systems, (1) the subtropical high pressure belt, which brings stable conditions to the country during the northern hemisphere winter, when the Inter tropical Convergence Zone (ITCZ) is displaced equatorwards, and (2) the the trade winds, which deliver summer rainfall to the central and southern regions of the country when the ITCZ shifts northwards [3]. Besides the shifts in the strength and location of these dominant atmospheric circulation systems,

orography is another key factor affecting the Mexican climatic conditions, although the elevation-climate relationship in Mexico is still an area that needs to be investigated in more detail.

ENSO is the most important climate phenomena at a global scale and has important effects in the precipitation of several parts of the world [4], exerting also influence in ecosystems or agriculture, among others [5]. Several works addressed the impact of ENSO on Mexican precipitation by using reanalysis data [6] or isolated observations [7, 8]. It was reported that above normal precipitation is experienced across the northern part of Mexico, while drier conditions prevail in the southern half of the country during El Niño years [6, 8]. In contrast, during the opposite phase of the ENSO phenomenon, La Niña, widespread wetter conditions are dominant throughout the tropical regions. Summer Mexican precipitation returns to their normals or even exceeds this threshold. Other works depicted a little different picture [7], during the summer months they identified a direct relationship between ENSO and precipitation in the northern part of Mexico and an inverse relationship in the part that lies south of latitude 22ºN. In the winter months, there is a general increase in precipitation with higher ENSO index values.

Overall, the ENSO phenomenon is an important factor that modulates the precipitation in Mexico. Unlike the Asian Monsoon where the variations in land–sea temperature contrast exert a strong control on the strength of the monsoon circulation, the mechanisms of rainfall interannual variability of the monsoonal climate of Mexico are not so well understood. The Southern Oscillation should exert a modulating influence on the Mexican precipitation throughout the year with two contrasting responses; extra-tropical conditions for the dry season and a tropical response in the boreal summer rainy period. However, although the study of moisture transport is probably the most powerful tool to understand the precipitation dynamics, the water vapor fluxes associated with the ENSO anomalies over Mexico have not been analyzed.

In this work, we first re-examine the regional influence of the ENSO over Mexico in terms of precipitation by using four different gridded rainfall data sets and three ENSO indices. Once the signal of ENSO over Mexico is established, the moisture transport anomalies associated with this signal are investigated, for improving our understanding of the interannual variability of precipitation regime over Mexico. Section 2 describes the datasets and the methodology. The ENSO-related interannual variability of precipitation over Mexico and the associated water vapor fluxes are discussed in section 3. A summary and the main conclusions are given in section 4.

2. Material and methods.

2.1. ENSO-related precipitation anomalies.

Four different sets of gridded monthly precipitation data are employed: (a) CHIRPS (Climate Hazards Group InfraRed with Station data) contains both sattelite and gauge station data, and posseses 0.25° x 0.25° spatial resolution with a 30 year time series from 1981-present [8]; (b) CMAP (Climate Prediction Center Merged Analysis of Precipitation) was build from gauge stations, ships, buoys and satellites. This data set has 2.5° x 2.5° spatial resolution with a 1979-2015 time series and is recommended to identify spatial and temporal precipitation variability in the tropics [9]; (c) GPCC (Global Precipitation Climatology Center) is based on gauge stations. It has an available time series from 1901-2013 with 0.5° x 0.5° spatial resolution. GPCC is recommended for global and regional water balance studies [10]; and (d) GPCP (Global Precipitation Climatology Project) has a 2.5° x 2.5° grid from 1979 – October 2015 [11]. The 34-yr common period for the dour databases 1981-2014 is studied.

In order to obtain robust results three ENSO indices are used in these work: (a) SOI (Southern Oscillation Index) is an index based on pressure differences between the East and West Pacific [12]; (b) ONI (Ocean Niño Index) monthly mean that takes sea surface temperatures anomalies every three months [13]; and (c) BEST (Bivariate EnSo Timeseries) which is based on a combined value between sea surface temperature and the SOI index [14]. Monthly precipitation composites for El Niño/La Niña indices above/below one standard deviation (the contrary for the SOI index) are assessed. The anomalies of these composites with respect to the rest of the 34-yr period are computed. Finally, the significance of composite differences is tested by the bootstrap method [15], where the original time series is permuted in a nonparametric bootstrap method to evaluate the statistical significance.

2.2 Moisture transport associated with ENSO rainfall anomalies.

The method developed by Stohl and James [16, 17] is employed in the present work to implement a dynamical analysis of the water vapor transport by using the Lagrangian particle dispersion model FLEXPART [18]. FLEXPART is driven with meteorological data from the European Centre for Medium-Range Weather Forecasts (ECMWF) [19]. They have a temporal resolution of 6 h and a horizontal resolution of 1°x1° on 60 levels. 3-D wind field is used to move roughly 2 million of so-called particles (air parcels) that result from the homogeneous division of the atmosphere. Further details of the model can be found in the FLEXPART technical note [20]. For each particle, the specific humidity (q) and position are stored at 6-h intervals. Changes in the specific humidity of the particle give the increases (e) and decreases (p) in moisture by the equation:

$$e–p = m\,(dq/dt)$$

where m is the mass of the particle and t is the time. The surface freshwater flux per unit area (E–P) is obtained at each grid position by adding (e–p) from all the air parcels located over it.

In order to delineate the regions affected by ENSO, composites for the three highest years of El Niño index minus the 3 highest years of La Niña are computed. After that, FLEXPART was run for these areas during a 34 year period (1981–2014).

3. Results and Discussion.

Figure 1 shows monthly anomalies during El Niño years (BEST index above one standard deviation) minus the remaining years for GPCC database. Positive anomalies can be seen in a reduced area over northwestern Mexico for March, and more widespread for May. Significant drier conditions begin to dominate throughout the southern Mexico in June, and they are clearly evident during July and August for the central and southern part of the country. These anomalies are again confined to the southern part in September. Significant drier conditions are present in Yucatan Peninsula for October. In November, wetter conditions appear, and they dominate over most of the country during the winter (December, January and February). Meanwhile, during the same season decreasing rainfall occurs in the most southern part (the Isthmus of Tehuantepec). Very similar results are obtained with the other three precipitation datasets and the other two ENSO indices (figures not shown), which makes the results very robust. Statistically significant anomalies with opposite signal for La Niña years are found as shown in figure 2.

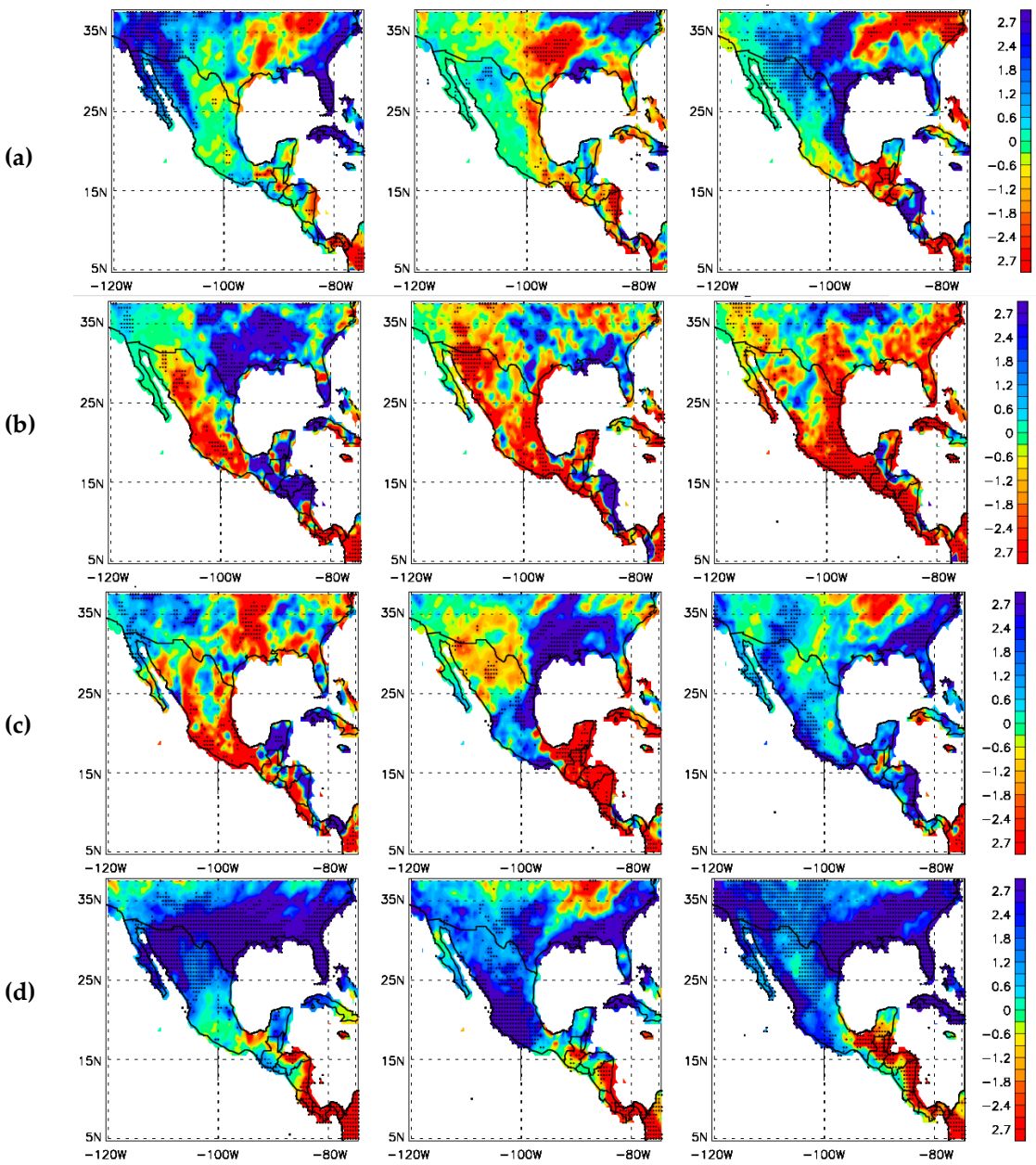

Figure 1. Precipitation anomalies (mm/day) during El Niño years for: (a) spring (March, April and May); (b) summer (June, July and August); (c) autumn (September, October, November) and (d) winter (December, January and February). The dotted areas indicate where the differences are significant at 95% confidence level, according to a bootstrap test.

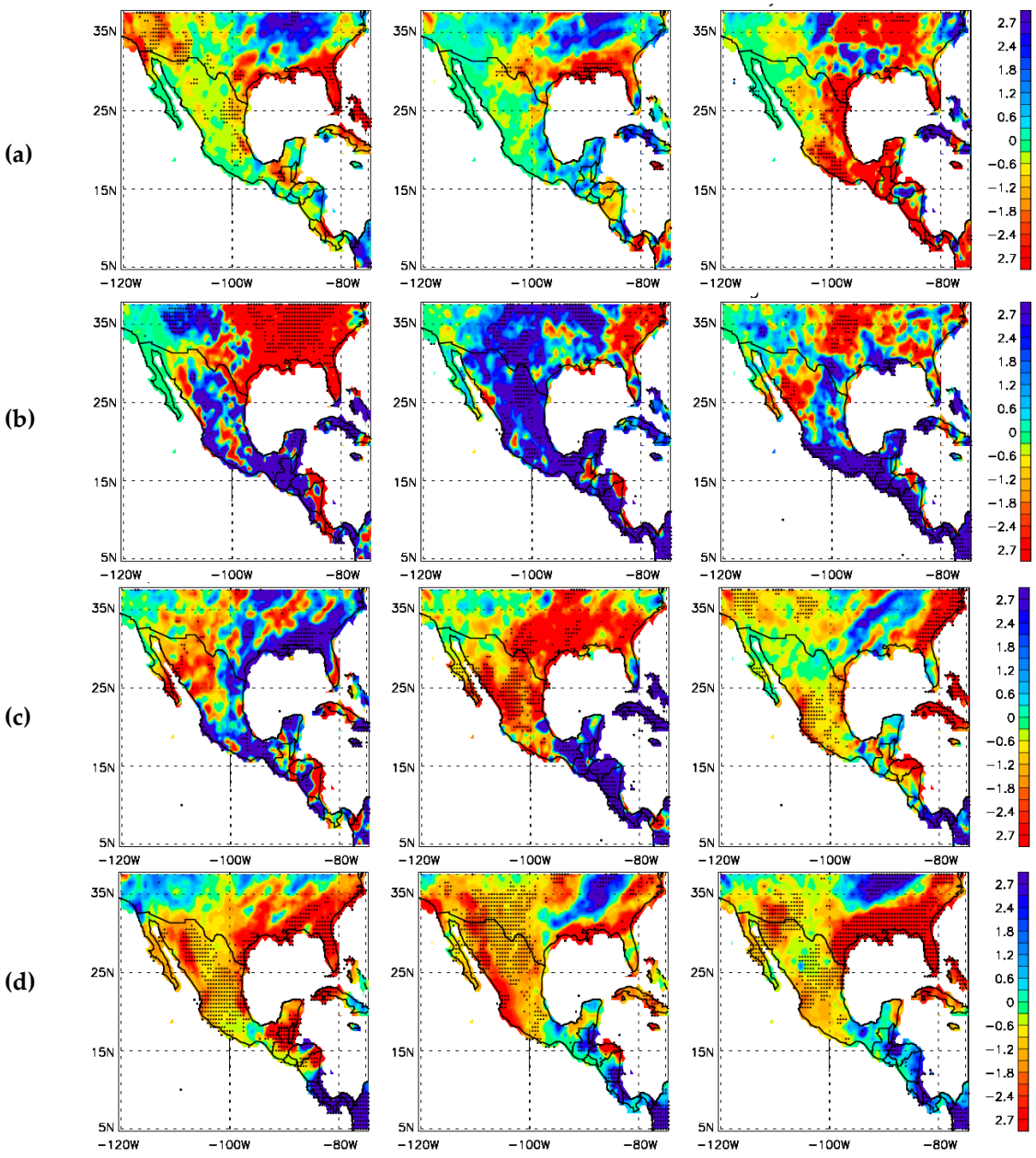

Figure 2. Precipitation anomalies (mm/day) during La Niña years for: (a) spring (March, April and May); (b) summer (June, July and August); (c) autumn (September, October, November) and (d) winter (December, January and February). The dotted areas indicate where the differences are significant at 95% confidence level, according to a bootstrap test.

Trying to find out some mechanism responsible for the above shown anomalies we have analyzed if there are any differences in the sources of moisture for the humidity that reaches the studied area. So, we select for winter and summer those areas that showed statistically significant anomalies of the three most strong El Niño events minus the three most strong La Niña events. These extreme years selected for both phases are concurrent in the different ENSO indices employed in this work. The boundaries and extension of these regions are presented in figure 3. As mentioned, ENSO impacts over northern Mexico in winter and over the central and southern part of the country in summer.

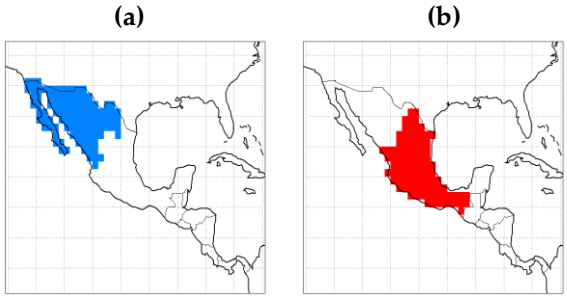

Figure 3. Geographic limits, and extent of the regions affected by ENSO during (a) winter (December, January and February), and (b) summer (July, August and September).

Figure 4 shows the seasonal average surface freshwater flux (E – P) agregated for the day -1 to the day -10 before the air mases aimed to both regions reach the areas, $(E - P)_{1\text{-}10}$ from now on, for the period 1981–2014. The 10-day limit was chosen as the average time of water residence of water in the atmosphere [21]. Moisture sources are those regions where the atmosphere gains humidity (reddish colors in figure 4), and moisture sinks are those where the water vapour is lost (bluish colors).

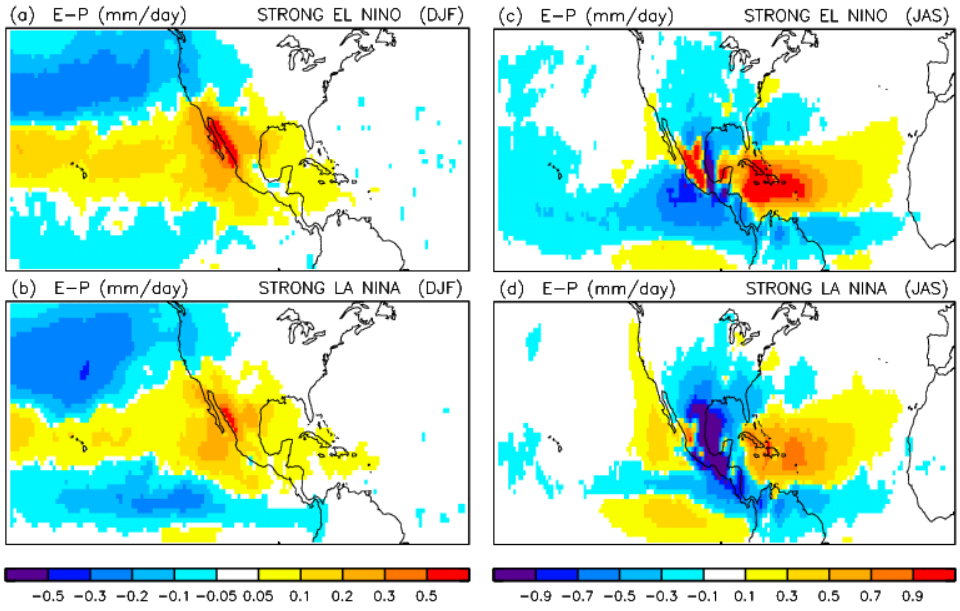

Figure 4. Composites of $(E\text{-}P)_{1\text{-}10}$ (mm/day) during winter for strong (a) El Niño, (b) La Niña, and during summer for strong (c) El Niño, (d) La Niña.

During strong El Niño winters (figure 4a), air masess from the Pacific Ocean aimed towards northwestern Mexico are characterized by higher positive values of $(E - P)_{1\text{-}10}$ than during the strong La Niña winters (figure 4b). ENSO shifts the path of the mid-latitude jet streams, which has a notable effect on the type of weather experienced in North America. During La Niña, the Pacific jet stream often meanders high into the North Pacific and is less reliable across the northern Mexico. In contrast, during an El Niño event in winter, the jet stream displaces to lower latitudes, typically moving the storm tracks, and thus the moisture, into southwestern USA and nortwestern Mexico, as was also pointed out by [6]. This is probably in the origin of ENSO-related anomalies of water vapor fluxes aimed toward northern Mexico.

During summer, the tropical Atlantic Ocean provides moisture to the central and southern Mexico, being this moisture amount higher for strong El Niño than for strong La Niña summer months (figures 4c and 4d). Over the Caribbean Sea, the low-level jet strengthens with El Niño [22], but the water vapor traveling in this easterly flow is apparently lost in the most western part of the Gulf of Mexico (figure 4c). During El Niño summers, the ITCZ remains closer to the eastern Pacific [23] and most of Mexico exhibits a relatively dry atmosphere (figure 4c). During La Niña an intense ITCZ forms around the equatorial latitude (figure 4d), allowing the occurrence of more frequent southerly moisture surges that produce enhanced precipitation over southern and central Mexico [in concordance with the ideas proposed in 6].

4. Conclusions

In this work, we first re-evaluate the regional influence of ENSO over the Mexican rainfall by using four differents gridded rainfall data sets and three different ENSO indices. Our results (which are in agreement with the scarce previous studies that used discrete observations or reanalysis data) show that during El Niño summers, negative precipitation anomalies dominate over most of Mexico. During La Niña the opposite pattern is found and precipitation exceeds the climatological mean. During winter air masess from the Pacific Ocean aimed towards northwestern Mexico are characterized by higher positive values of $(E - P)_{1\text{-}10}$ during El Niño than during La Niña, likely because the Pacific jet stream shift southward the north of Mexico latitudes. In spring and autumn Mexican precipitation does not present a quite significant signal.

The moisture transport that provoques these rainfall anomalies, has been computed thoughtout a lagrangian approach. The obtained (E - P) patterns are in consistent with rainfall anomalies and in concordance with several mechanisms proposed in the literature. Therefore, a deep analysis of these patterns seems to be a good approach to unveil the mechanisms that control the ENSO-related mexican rainfall interannual variability.

Acknowledgments

This research is a contribution to the project PAPIIT IA103116.

Author Contributions

Paulina Ordoñez and Pedro Ribera conceived and designed the experiments; Ana E. Melgarejo, Raquel Nieto and Luis Gimeno performed the experiments; and Ana E. Melgarejo analyzed the data; Ana E. Melgarejo and Paulina Ordoñez wrote the paper.

Conflicts of Interest

The authors declare no conflict of interest.

References

1. Mosiño, P.A., Garcia,E. (1974). The climate of Mexico. R.A. Bryson y F.K. Hare (Ed), Elsevier Sci. Pub. Co., 345-391.
2. Jáuregui, E. (1997). Climate changes in Mexico during the historical and instrumented periods. *Quaternary Int.* 43: 7-17.
3. Endfield, G.H. (2008). Climate and Society in Colonial Mexico. A study in vulnerability. Royal Geographycal Society. Blackwell publishing. ISBN 978-1-4051-4582-4.
4. Ropelewski, C., Halpert, M. (1987). Global and regional scale precipitation patterns associated with El Niño/Southern Oscillation. *Monthly Weather Review*, 1606-1626.
5. Cai, W. and Co-authors. (2014). Increasing frequency f extreme El Niño events due to greenhouse warming. *Nature climate change*, 111-116.

6. Magaña, V., Vázquez, J., Pérez, J., Pérez, J. (2003). Impact of El Niño on precipitation in Mexico. *Geofisica Internacional-Mexico*, 313-330.
7. Bravo-Cabrera, J.L., Azpra-Romero, E., Zarraluqui-Such, V., Gay-García, C. (2017). Effects of El Niño in Mexico during rainy and dry seasons: an extended treatment. *Atmósfera*, 30 (3): 221-232.
8. Funk, C.C., Peterson, P.J., Landsfeld, M.F., Pedreros, D.H., Verdin, J.P., Sukla, S., Husak, G.J., Rowland, ,JD,, Harrison, L., Hoell, A., Michaelsen, J.C. (2015). The climate hazards infrared precipitation with stations- a new enviromental record for monitoring extremes. Scientific Data 2. 630 doi:10.1038/sdata.2015.66.
9. Arkin, Phil, Xie, PIngping and National Center for Atmospheric Research Staff (Eds). Last modified 13 Oct 2017. "The Climate Data Guide: CMAP: CPC Merged Analysis of Precipitation". Retrieved from https://climatedataguide.ucar.edu/climate-data/cmap-cpc-merged-analysis-precipitation.
10. Schneider, Udo; Becker, Andreas; Finger, Peter; Meyer-Christoffer, Anja; Rudolf, Bruno; Ziese, Markus (2015). GPCC Full Data Reanalysis Version 7.0 at 1.0°: Monthly Land-Surface Precipitation from Rain-Gauges built on GTS-based and Historic Data. DOI: 10.5676/DWD_GPCC/FD_M_V7_100.
11. Adler, R.F., G.J. Huffman, A. Chang, R. Ferraro, P. Xie, J. Janowiak, B. Rudolf, U. Schneider, S. Curtis, D. Bolvin, A. Gruber, J. Susskind, and P. Arkin (2003). The Version 2 Global Precipitation Climatology Project (GPCP) Monthly Precipitation Analysis (1979-Present). J. Hydrometeor., 4,1147-1167.
12. http://www.cpc.ncep.noaa.gov/data/indices/Readme.index.shtml#SOICALC
13. http://origin.cpc.ncep.noaa.gov/products/analysis_monitoring/ensostuff/ONI_v5.php
14. https://www.esrl.noaa.gov/psd/people/cathy.smith/best/
15. Efron, B. and Tibshirani, R. (1993). An introduction to the Bootstrap Chapman and Hall New York Google Scholar.
16. Stohl A, James P. 2004. A Lagrangian analysis of the atmospheric branch of the global water cycle. Part 1: Method description, validation, and demonstration for the August 2002 flooding in central Europe. *Journal of Hydrometeorology*, 5: 656–678.
17. Stohl A, James P. 2005. A Lagrangian analysis of the atmospheric branch of the global water cycle. Part 2: Earth's river catchments, ocean basins, and moisture transports between them. *Journal of Hydrometeorogy*, 6: 961–984.
18. Stohl A, Hittenberger M, Wotawa G. 1998. Validation of the Lagrangian particle dispersion model FLEXPART against large scale tracer experiment data. *Atmospheric Environment* 32: 4245–4264.
19. Uppala, S.M. and Co-authors (2005). The ERA-40 re-analysis. *Q. J. R. Meteorol. Soc*. 131: 2961–3012.
20. Stohl A, Forster C, Frank A, Seibert P, Wotawa C. 2005. Technical note: The Lagrangian particle dispersion model FLEXPART version 6.2. *Atmospheric Chemistry and Physics* 5: 2461–2474
21. Numaguti A. (1999). Origin and recycling processes of precipitating water over the Eurasian continent: Experiments using an atmospheric general circulation model. *Journal of Geophysical Research* 104: 957–1972.
22. Amador, J.A., Magaña, V. (2000). The low-level jet and convective activity in the Caribbean. Reprints of the 24th Conference on Hurricanes and Tropical Meteorology. Ft. Lauderdale, Fla. 29 May – 2 June, 2000, 114-115.
23. Waliser, D.E., Gautier, C. (1993). A satellite derived climatology of the ITCZ. *J. Climate., 6*, 2162-2174.